Single and Multitransfer Reactions Induced by 86-MeV ^{12}C Ions on Silver Nuclei

J. GALIN, B. GATTY, M. LEFORT, J. PETER, AND X. TARRAGO
Laboratoire de Chimie Nucléaire, Institut de Physique Nucléaire, 91 Orsay, France
AND
R. BASILE
Faculté des Sciences d'Orléans, Orléans, France
(Received 24 February 1969)

Heavy particles from silver targets bombarded by ^{12}C heavy projectiles have been identified using a counter telescope and bidimensional analysis of ΔE and E data. Energy distributions have been measured for Li, Be, B, C, N, and O nuclei. Angular distributions exhibit a maximum which is related to the distance of closest approach. The largest cross sections are observed for ^{11}B $(-1p)$ and ^{13}C $(+1n)$ single transfer. It is emphasized that the total cross section for the loss of a proton by the projectile is 60 times the cross section for the pickup of a proton. The products of transfer reactions are mainly formed in excited states, but the angular distribution does not depend on the degree of excitation, at least for the lowest excited states.

1. INTRODUCTION

NUCLEON transfer reactions with heavy projectiles ($Z>2$) have been studied mostly on light targets in order to investigate their nuclear structure. The few studies made on medium and heavy targets, done radiochemically, have been concerned with neutron transfers. A large amount of work has been presented in 1960 and 1963 at the conferences on reactions between complex nuclei,[1] and it was shown that for energies near the Coulomb barrier and for light targets, the "tunneling" theory of Breit and co-workers[2] provides a good explanation of most of the results, both for proton and neutron transfers. The theory proposes essentially that the nuclei travel on classical Rutherford scattering trajectories before and after the reaction. The transferred nucleon tunnels from one nucleus to the other and the largest probability is obtained at the distance of closest approach $R_{\min}=Z_1Z_2e^2/2\bar{\epsilon}[1+\csc(\bar{\theta}/2)]$, where Z_1 and Z_2 are the atomic numbers of the interacting nuclei, e is the electronic charge, $\bar{\epsilon}$ is the center-of-mass energy, and $\bar{\theta}$ is the center-of-mass angle.[3]

But, at higher energies, large discrepancies occur. Also more recent works have shown that proton and neutron transfers behave very differently.[4] On heavy targets, the yields are much lower for proton cases than for neutron cases and some radiochemical studies have shown that the loss of protons by the target appeared to be much less probable that the corresponding gain of protons. In other words, it seems much easier for the projectile to lose one proton than to pick up one proton. Very recently, Diamond *et al.*[5] have used a power-law type particle-identifier system with semiconductor detectors, in order to study the one-proton transfers on several targets. They measured, for example, the ratio ^{12}C to ^{10}Be using ^{11}B projectiles. The observation of the new ion was done more or less at the grazing angle. These authors found (i) that the proton transfer cross sections dropped by a factor of 2 or 3 as the Z of the target increased from Ni to Au, and (ii) that the ratio $\sigma(+p)/\sigma(-p)$ of the yield of one proton transferred into the projectile to that of one proton transferred out of the projectile decreased a factor of 5 as the Z of the target went from 28 to 79. They proposed that these two features can be understood by considering the relevant potential energies of the systems, which have been approximated by the masses at infinite separation (Q_0 values), plus a Coulomb interaction energy term important for heavy projectiles and targets.

In the year 1960, an additional phenomenon was discovered: multinucleon transfer, which occurs at higher bombarding energies. Although the one-nucleon transfer levels off at some 20–30 mb for 10 MeV per nucleon, the yield for multinucleon transfer still increases at this energy. Kaufman and Wolfgang[6] have studied the angular distribution for losses from projectile of $(p2n)$, $(2p3n)$, $(2p4n)$, $\cdots$, and pick up by projectile of (pn), $(2p2n)$, $(3p3n)$. None of them presented a critical angle at which the differential cross section reached its largest value, and multinucleon transfer products were always peaked near or at 0°. The explanation given at that time was the "grazing contact mechanism." In a grazing trajectory, when the two

[1] *Proceedings of the Second Conference on Reactions between Complex Nuclei, Gatlinburg 1960,* edited by A. Zucker, E. C. Halbert, and F. T. Howard (Wiley-Interscience, Inc., New York, 1960); *Proceeding of the Third Conference on Reactions between Complex Nuclei, Asilomar, 1963,* edited by A. Gheorso, R. M. Diamond, and H. E. Conzett (University of California Press, Berkeley, 1963).
[2] G. Breit and M. E. Ebel, Phys. Rev. **103**, 679 (1956); **104**, 1030 (1956); G. Breit, in *Handbuch der Physik*, edited by S. Flugge (Springer-Verlag, Berlin, 1959), Vol. 41.
[3] J. A. McIntyre, T. L. Watts, and F. C. Jobes, Phys. Rev. **119**, 1331 (1960).
[4] V. V. Volkov and J. Wilchynski, Nucl. Phys. **92**, 495 (1967).
[5] R. M. Diamond, A. M. Poskanzer, F. S. Stephens, W. J. Swiatecki, and D. Ward, Phys. Rev. Letters **20**, 802 (1968).
[6] R. Kaufmann and R. Wolfgang, Phys. Rev. **121**, 192 (1961).

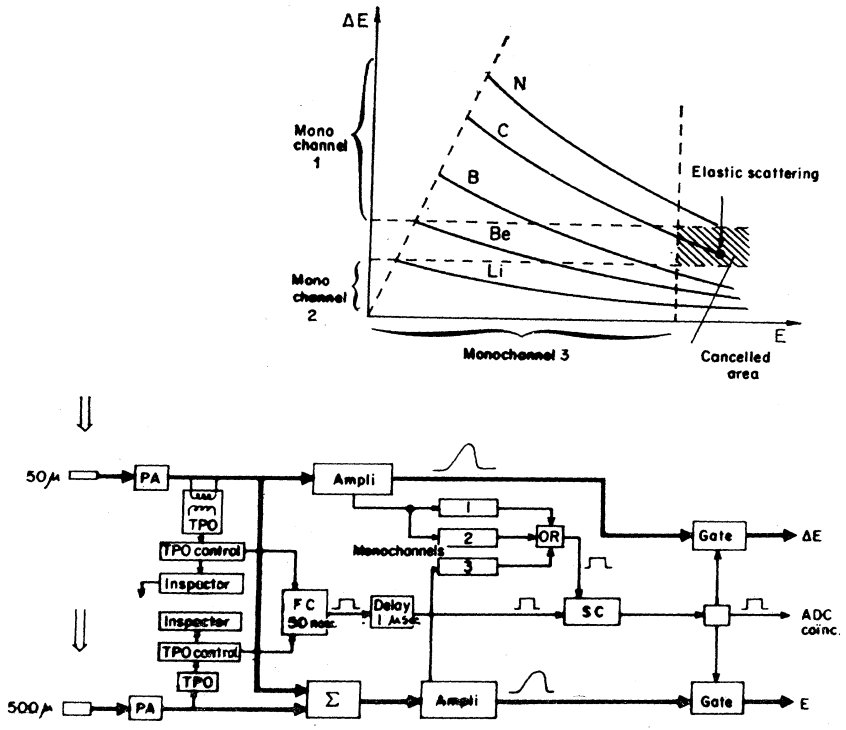

FIG 1. Electronic block diagram and ΔE versus E relationships.

nuclei come in contact, transfer of clusters of nucleons take place. As the volume of contact is excited, the complete amalgamation of target and projectile is avoided because the bond between them is kept weak. After a transitory coupling, the remaining forward momentum plus the Coulomb repulsion causes a separation. The final product may have the same number of nucleons as the projectile, more, or fewer. The transformed incident ion continues its motion essentially on a trajectory with a very small deflection angle.

However, subsequent experiments have shown that angular distributions from multinucleon transfers do not always display a monotonic increase in the differential cross section as the angle decreases. Kumpf and Donetz[7] have found maxima similar to those observed in single-nucleon transfers in their studies of reactions induced on ^{232}Th by ^{22}Ne ions. The same result was obtained recently by Volkov *et al.*[8] for the transfer of ^{4}He from ^{12}C and ^{14}N to gold targets at about 40°. Also, Lozynski,[9] in his investigation of reactions induced on gold by 140-MeV ^{20}Ne, found three peaks in the angular distribution. Wilczynski, Volkov, and Decovski[10] have tried to distinguish between a quasi-elastic and an inelastic process, by considering, in the energy distribution of the transformed ions, a part corresponding to a ground state and a part corresponding to excited states. However, the separation was purely arbitrary.

It seemed to us indeed interesting to study separately angular distributions for the cases in which the new ion is left in its ground state, i.e., when its kinetic energy corresponds to the calculated Q_0 value (difference of masses) considering the kinematical conditions at a given angle, and for the cases in which the new ion is excited to a given level. Therefore, we thought that we needed a good energy resolution which could not be obtained by radiochemical technics. Also, our wish was to detect at the same time all the possible ions produced at a given angle, in order to investigate in identical conditions both neutron and proton single transfers and various multitransfer reactions. We believed that the best method was to identify and measure the energy of the ions using a counter telescope. The experiments we are going to describe were done with ^{12}C projectiles (86 MeV) on a natural-silver target. They are the first of a series in which we intend to vary the energy, the nature of the projectile and the nature of the target. Silver was chosen because of the ease in making thin targets. It is true that having equal proportions of the two isotopes 107 and 109 is a disadvantage. However, we believe that the results depend to a rather small extent on the structure of the target provided that its Z number is large enough.

[7] H. Kumpf and E. D. Donetz, Zh. Eksperim. i Teor. Fiz. **44**, 798 (1963) [English transl.: Soviet Phys—JETP **17**, 539 (1963)].
[8] V. V. Volkov, G. F. Gridnev, G. N. Zorin, and L. P. Chelnokov, Joint Institute for Nuclear Research Report No. E-7-4071, Dubna, 1968 (unpublished), Nucl. Phys. **A126**, 1 (1969).
[9] E. Lozynski, Nucl. Phys. **64**, 321 (1965).
[10] J. Wilczynski, V. V. Volkov, and P. Decovski, Yadern Fiz. **5**, 942 (1967) [English transl.: Sov. J. Nucl. Phys. **5**, 672 (1967)].

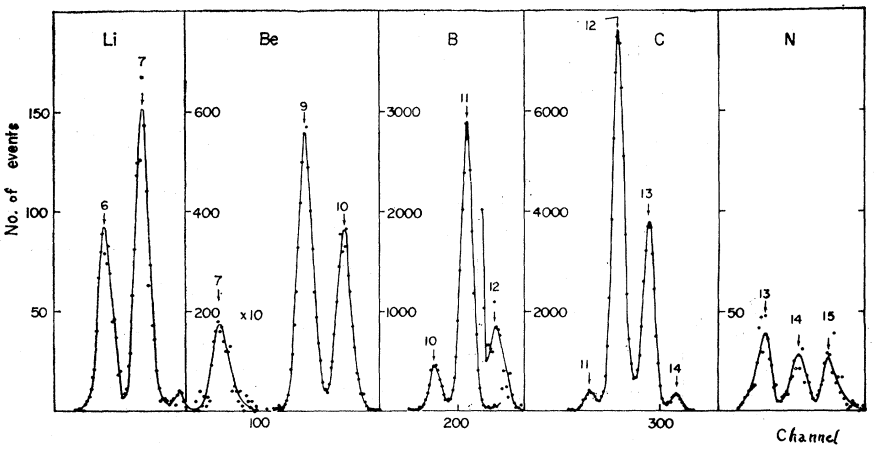

FIG. 2. Mass spectrum obtained at $\theta_L=30°$. Mass and Z numbers (in abscissa channel numbers) are given on each peak.

2. EXPERIMENTAL DEVICE FOR IDENTIFICATION OF PRODUCTS

Heavy particles ($Z>2$) from the target were identified by two surface-barrier solid-state detectors. The front one, entirely depleted, was 50 μ thick and measured $\Delta E/\Delta x$. In the back, a second junction 450 μ thick stopped all heavy particles entering through the first detector with a sufficient energy. The aperture was defined by a diaphragm of 4 mm diam placed in front of the first junction, at 30 cm from the target. A thin aluminium foil, 1 μ thick, protected the detectors against the slow electron flux emitted by the bombarded target. The absolute intensity of the beam was measured by a Faraday cup. A crystal was also put above the beam at an angle of 40°, and was used as a monitor by counting carbon ions which were elastically scattered.

As is shown on the electronics block diagram in Fig. 1, signals from the detectors followed a linear chain and a logical chain. In the linear chain of the $\Delta E/\Delta x$ detector, the charge preamplifier delivered a signal with a very short rise time (10^{-8} sec) which entered into an amplifier where it was shaped. The signal from the amplifier passed through a gate to the analog-digital converter (ADC) ΔE. The same pulse was also taken at the output of the preamplifier and its height was added to the E detector pulse height in a linear sum circuit. The signal delivered by the sum circuit was shaped and entered the ADC No. 2 (E converter) after passing through a gate. Both gates ΔE and E were opened by pulses coming from the logical chain.

The origin of the logical chain was made of two time pickoff (TPO) circuits associated with the two preamplifiers. The pulses were very strongly differentiated by a 3.10^{-9}·sec line. Then they passed through the TPO device in such a way that it allowed low thresholds for the pulse height (corresponding to a 3-MeV deposit in the first detector and 1-MeV in the second one) and, therefore, a very wide scale (between 1 and 80 MeV). Time fluctuations from one signal to the other were shorter than 10^{-8} sec. Pulses delivered by TPO circuits were sent into a fast coincidence circuit ($2\tau=6.10^{-8}$ sec). The outgoing pulse entered into a slow coincidence circuit ($2\tau=5.10^{-7}$ sec) as well as a signal resulting from 3 monochannel selectors. Such a device allowed, when it was desirable, to get rid of the counting of very numerous events corresponding to elastic scattering, as shown briefly on the diagram of Fig. 1.

The pulse delivered by the slow coincidence circuit was used to open the gates on the two linear chains. Every event was coded as two numbers, each with 10 bits (1024 per 1024 channels), and was stored in two buffer memories containing 256 positions each. The contents of these memories were alternately transferred to a magnetic tape. Magnetic tapes were afterwards treated on an UNIVAC 1108 computer in order to obtain for each event the mass, the atomic number, and the energy of the particle detected.

The Z identification was done easily by a comparison of the product $E\times\Delta E$ of the data from each event with the possible values of $E\times\Delta E$ corresponding to a particular Z in the $E\times\Delta E$ plane.

The mass identification was more difficult. After several trials, we decided to use the range energy relationships. We called $R(E, M)$ the range in Si of an ion of mass M and energy E. For a given mass M_0, we had at our disposal the experimental data from Northcliffe[11] on range energy relationships $R_{M_0}(E)$. The curve was expressed by an hyperbolic function $\alpha_1E^2+\alpha_2R^2+\alpha_3ER+\alpha_4E+\alpha_5R+\alpha_6=0$. The coefficients were determined by taking 5 points on the curve.

Now, for any mass M of the same Z, we could express $R_M(E)$ in the form $R_M(E)=R_{M_0}(E)+F(E, M)$, where $F(E, M)$ is a function equal to zero for the particular value M_0. Furthermore, we have made the assumption, suggested by an analysis of Northcliffe's curves and justified afterwards by our results, that $F(E, M)$ can be expressed as a product of two func-

[11] L. C. Northcliffe, Phys. Rev. **120**, 1744 (1960); Ann. Rev. Nucl. Sci. **13**, 67 (1963).

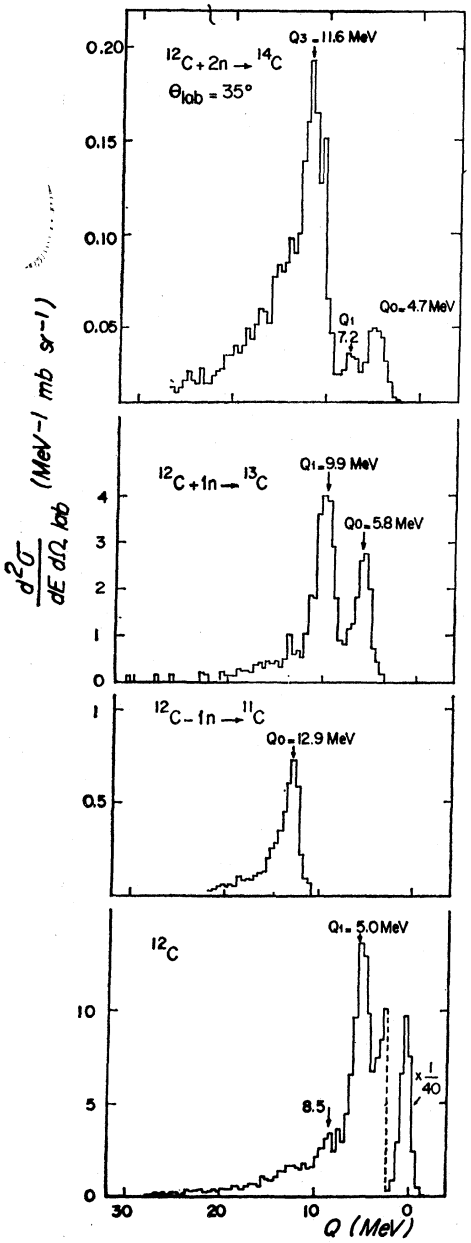

FIG. 3. Energy distribution for ^{11}C, ^{12}C, ^{13}C, and ^{14}C ions. In abscissa, Q values are plotted from right to left.

tions with separated variables: $F(E, M) = S(E)G(M)$. The way to determine the function $S(E)$ was to take a new particular mass, M_1, next to M_0, and to use again Northcliffe's curve: We can write

$$R_{M_1}(E) = R_{M_0}(E) + S(E)G(M_1),$$

where $G(M_1)$ is now a constant. We have chosen it equal to 1. Again the experimental curve for R_{M_1} against E could be expressed by an hyperbolic function and $S(E) = R_{M_1}(E) - R_{M_0}(E)$ was obtained along all the energies. If we call T the thickness of the $\Delta E/\Delta x$ detector, it can be expressed as $T = R(E) - R(E-\Delta E)$, where $R(E)$ is the range in Si of a particle of mass M and energy E and $R(E-\Delta E)$ is the range in the second detector of the same particle which has lost ΔE in the first detector.

Expressing as above $R(M, E) = R_{M_0}(E) + S(E)G(M)$, we had $T = R_{M_0}(E) + S(E)G(M) - R_{M_0}(E-\Delta E) - S(E-\Delta E)G(M)$ and, therefore, we obtained for each mass M the particular values of $G(M)$,

$$G(M) = (T + R_{M_0}(E-\Delta E) - R_{M_0}(E))/(S(E) - S(E-\Delta E)).$$

It should be noted that $G(M)$ is equal to zero for the mass M_0 and is equal to 1 for mass M_1. Functions R and $S(E)$ have been established with the help of Northcliffe's curves for all Z values between Li and O. Then it was easy on the computer to make a program which recognized all the events and which attributed them to different masses. For a given mass M_i, we have checked that all the events were accumulated in an area very closed to an horizontal line when $G(Mi)$ is plotted versus the energy E. The good separation between two $G(M)$ is demonstrated in Fig. 2.

If one compares the previous method with a particle identifier, it has the great advantage to be valuable over a very wide range of energies from 10 to 100 MeV and a very large range of masses from 6 to 16.

3. EXPERIMENTAL RESULTS: MASS SPECTRA AND ENERGY DISTRIBUTIONS

Mass spectra have been obtained at angles θ, 25°, 30°, 35°, 40°, 45°, and 55° in the laboratory system. An example of a mass spectrum taken at $\theta = 30°$ is illustrated in Fig. 2. The separation of each mass can be readily done and it is shown that ^6Li and ^7Li, ^7Be, ^9Be, and ^{10}Be, ^{10}B, ^{11}B, and ^{12}B, ^{11}C, ^{12}C, ^{13}C and ^{14}C, ^{13}N, ^{14}N, and ^{15}N are very well identified. A very small number of counts were found in the area devoted to O ions and we can give the very low value of 10^{-30} cm^2 for the upper limit of the cross section for ^4_2He transfer reactions from the target to the projectile.

Therefore, the observed pick up by ^{12}C ions were $(+p2n)$ giving ^{15}N, $(+pn$, or $d)$ giving ^{14}N, $(+p)$ giving ^{13}N, $(+2n)$ giving ^{14}C, and $(+n)$ giving ^{13}C. ^{12}C ions were stripped of $(-1n)$ leading to ^{11}C, $(-p)$ leading to ^{11}B, $(-d$ or $pn)$ leading to ^{10}B, $(-2p)$ leading to ^{10}Be, $(-2pn)$ leading to ^9Be, $(-\alpha n)$ leading to ^7Be. A charge-exchange process might be responsible for the formation of ^{12}B and it is difficult to suggest a definite mechanism for ^6Li and ^7Li although one might think of a breakup of ^{12}C.

For each nucleus, an angular distribution $d\sigma/d\Omega$ versus $\bar{\theta}$ has been drawn in the center of mass, but we shall come back later to this aspect.

At a given angle, we have measured as accurately as possible the energy distribution. In most of the cases, an energy resolution of 700 keV was achieved

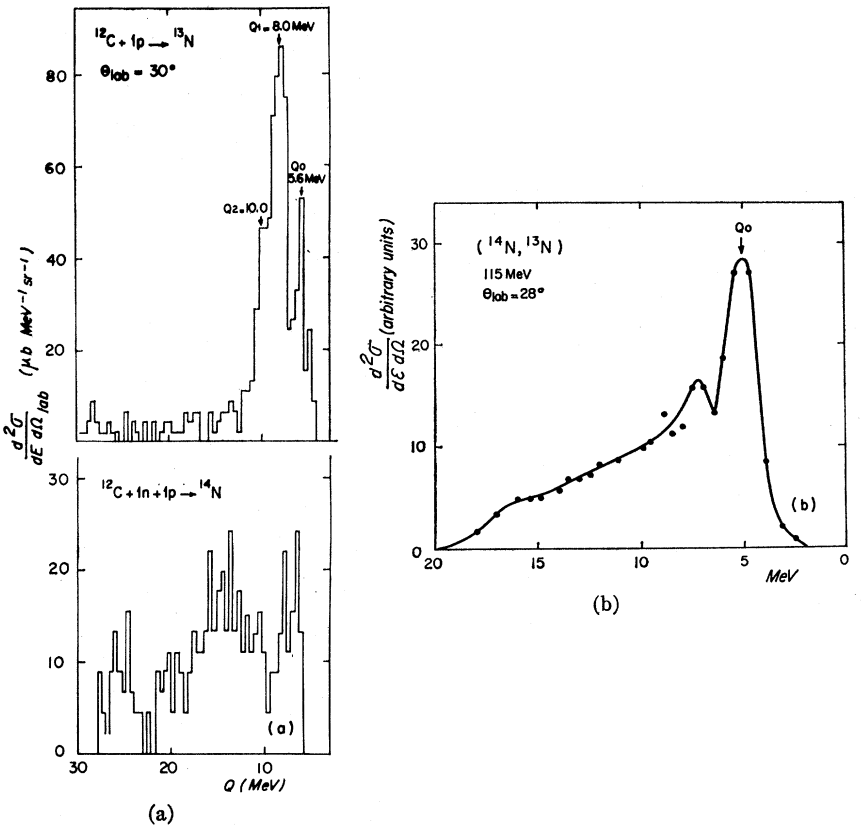

FIG. 4. (a) Energy distributions for ^{14}N and ^{13}N produced by ^{12}C projectiles. (b) Energy distribution for ^{13}N produced by ^{14}N projectiles.

and interesting energy spectra were found. Instead of a presentation of $d^2\sigma/d\epsilon\,d\Omega$ versus the kinetic energy of the observed ion, we have used on the abscissa scale a quantity related to the excitation energy. The Q value deduced from a measured kinetic energy of a particular ion at a given angle θ was calculated with the relation

$$\epsilon_i = \epsilon_i' + \epsilon_R + Q,$$

when ϵ_i is the incoming ^{12}C kinetic energy, ϵ_i' the measured kinetic energy of the product, ϵ_R the recoil energy calculated through the momentum conservation relationship. Then Q included any sort of energy which did not appear in the linear kinetic energy. If the new product was left in its ground state and if no rotation energy was transferred, $Q = Q_0$ was the mass balance of the reaction. It is possible to recognize directly in the energy spectra the location of a peak and to attribute it, for example, to the scattered ion and the recoiling nucleus both in their ground states. Alternatively, a peak may be attributed to the ion or the nucleus, or both, in excited states. With this analysis, the energy position of each peak was located at the same values for all detection angles.

Experimental energy spectra shown in Figs. 3–6 exhibit very clearly several peaks. Because the levels in Ag are closely spaced, it has been possible in most of the cases to distinguish the ground state and a few known levels of the final N, C, or B nucleus. In all the cases where the ground state could be clearly distinguished, its magnitude was much smaller than the amount of other states. In other terms, nuclei N 13 and 14, C 11, 13, and 14, and B 11 are mostly left in excited states after the transfer process. Now we would like to describe some particularities for each energy distribution.

The spectrum of ^{12}C exhibits below the very high elastic scattering peak, another peak at 5 MeV which corresponds to the well-known 2+ level of 4.43 MeV. A third peak at 8.5 MeV might be attributed to the fast decay from several levels of ^{13}N which are unstable with respect to proton emission and were measured by the detectors as ^{12}C ions.

The ground states for ^{13}C should be observed at $Q_0 = 5.1$ MeV and $Q_0 = 4.6$ MeV, for ^{107} Ag and ^{109}Ag, respectively. The first peak was indeed noticed around 5.8 MeV. Another maximum at 9.9 MeV might be due to the 3.09 and 3.68 excited levels.

Outside of the ground state, located at approximately 5.5 MeV, two excited levels of ^{13}N at 2.3 and 3.5 MeV could be responsible for experimental peaks at 8 and 10 MeV. As we have already mentioned, higher levels are known to be proton unstable; ^{13}N excited nuclei disintegrate before their detection and should have been measured as ^{12}C.

Several excited levels were also observed in ^{14}C and

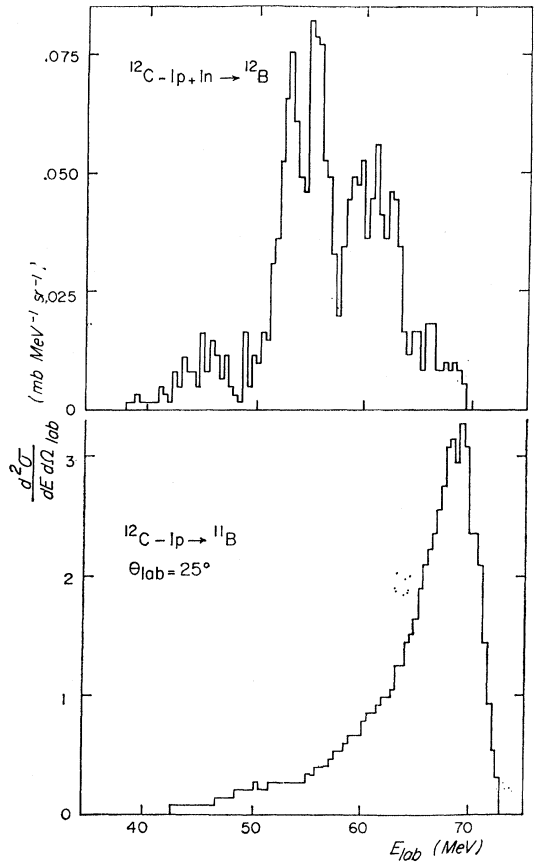

FIG. 5. Energy distributions for ^{12}B and ^{11}B.

^{14}N in addition to the ground-state peaks. As a general remark, the products of pickup processes (heavier than the projectile) showed spectra with several peaks. In contrast, energy distributions for the products of stripping (lighter than the projectile) were smooth curves without structure. This can be well understood since excited levels free for picking up a new nucleon are well defined and separated by large gaps, although the loss of nucleons may correspond either to the filling of any of the numerous excited levels in Ag, or to their departure as free entities. The number of open channels is therefore, very large. In this regard, it is interesting to compare energy distributions for ^{13}N produced either in a pickup process ($^{12}C+p$) or in a stripping process ($^{14}N-n$). Very recent experiments have been done with N ions on Ag and both spectra are given in Fig. 4(b). It is clear that the important point is the way followed by the transfer reaction and *not* its final product.

For a very large number of transferred nucleons, the energy distribution was spread over a wide range between the ΔE detector threshold and a maximum kinetic energy corresponding to the mass balance Q_0. Spectra for ^{7}Li, ^{9}Be, and ^{10}B are given in Fig. 6.

4. ANGULAR DISTRIBUTIONS AND STUDY OF TRANSFER MECHANISMS

Differential cross sections were found to be negligible at angles larger than 50°. Because of experimental difficulties due to the large yield of elastic scattering, the limit in the forward angles was 25°. We have been able, since these experiments, to measure ions down to 8°, but the new results will be published later on. Angular distributions between 25° and 55° were ob-

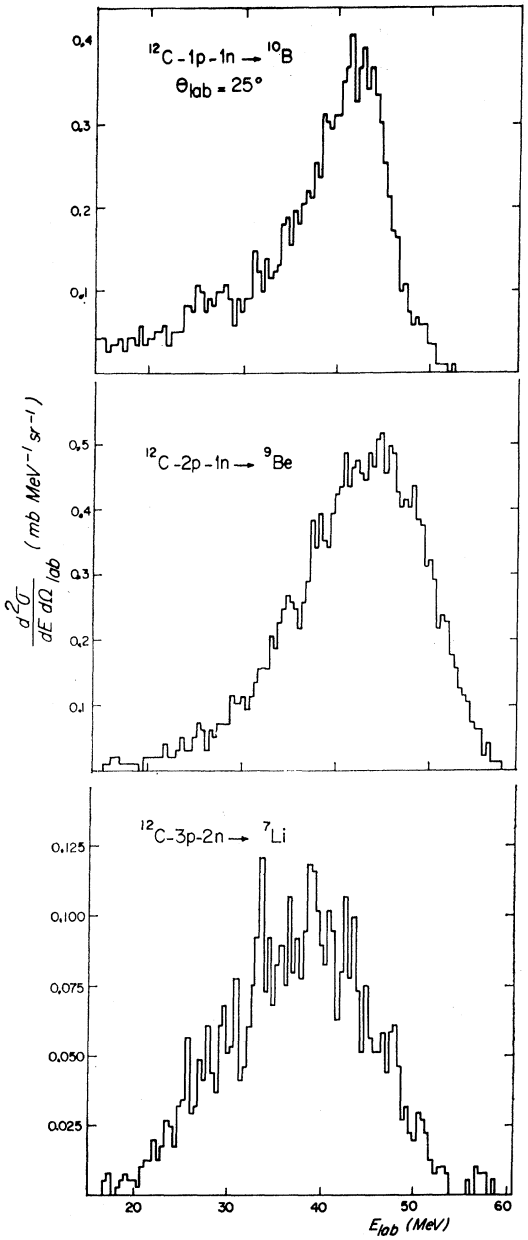

FIG. 6. Energy distributions for ^{7}Li, ^{9}Be, and ^{10}B (large multi-transfer reactions).

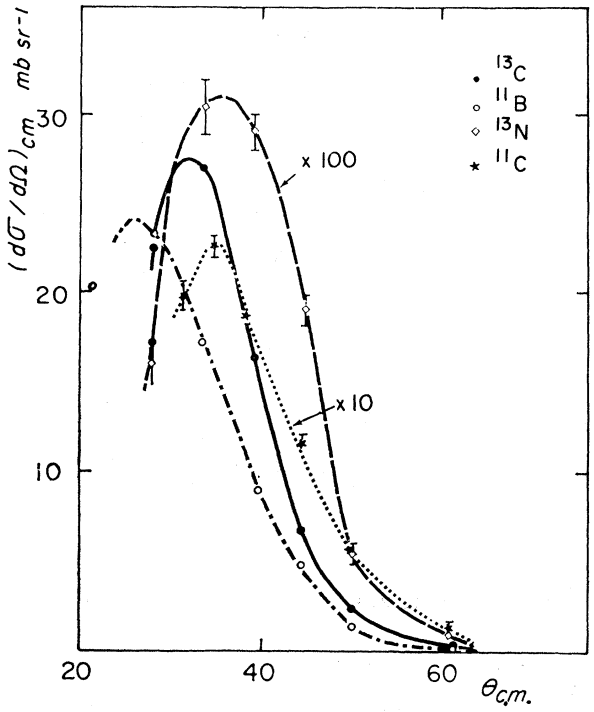

FIG. 7. Angular distributions for single-nucleon transfers in the center-of-mass system. ^{13}C, ^{11}C, ^{13}N, ^{11}B.

tained for each transfer reaction. When, in the energy distribution, several peaks could be clearly isolated, an angular distribution has been drawn for each peak. To our knowledge, such distributions have never been published before and we thought that an interesting problem was to know if a particular excited state of the nucleus behaved like the ground state. Some distributions are shown in Figs. 7–9. A somewhat different presentation of angular distributions transfer reactions is to plot, instead of $d\sigma/d\Omega$ versus $\bar{\theta}$ in the center-of-mass system, $d\sigma/dR_{\min}$ versus $R_{\min}$, where $R_{\min}$ is the distance of closest approach related to the Rutherford scattering angle

$$\frac{d\sigma}{dR_{\min}} = \frac{d\sigma}{d\Omega}\frac{d\Omega}{d\theta}\frac{d\theta}{dR_{\min}}.$$

Since

$$\frac{dR_{\min}}{d\theta} = -\tfrac{1}{4}b\frac{\cos\frac{1}{2}\bar{\theta}}{\sin^2\frac{1}{2}\bar{\theta}},$$

$$\frac{d\sigma}{dR_{\min}} = \frac{16\pi}{b}\frac{d\sigma}{d\Omega}\sin^3\tfrac{1}{2}\bar{\theta},$$

where b is related to the impact parameter p: $b = 2p\tan\frac{1}{2}\bar{\theta} = Z_1Z_2e^2/\bar{\epsilon}$.

Such an analysis shows in a straightforward manner the value of $R_{\min}$ at which the transfer process occurs with the largest probability. However, its correct application should take account of the fact that $\bar{\theta}$ is the angle at which the *final ion* is scattered, whereas the charge Z_1 and the reduced mass μ included in b belong to the *initial* projectile. In other terms, the analysis is done for a pure Rutherford scattering of the projectile, although the transfer of nucleons may have changed the ratio μ/Z_1 and the recoil nucleus charge Z_2.

This is the reason why we have programmed on a computer a more elaborate calculation for $R_{\min}$ values, which is based on a simplified model of trajectories shown in Fig. 10. When a projectile of kinetic energy

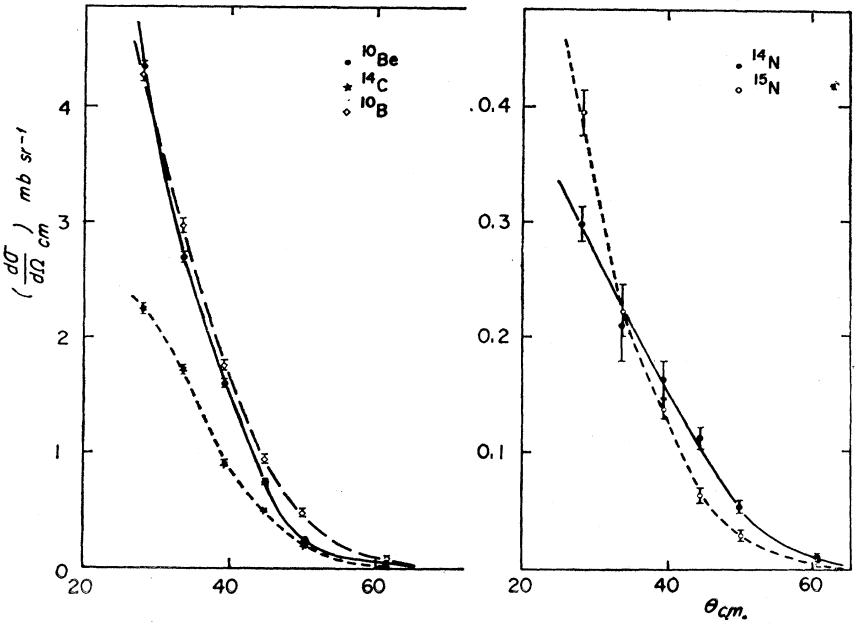

FIG. 8. Angular distributions for multitransfers.

$\epsilon_i = \frac{1}{2}m_1 v_1^2$ and impact parameter p is scattered by the target nucleus, it follows an hyperbolic trajectory in the center-of-mass system. The transfer reaction occurs at $R_{\min}$ and it is assumed that the Q value of the reaction affects the magnitude but *not the direction* of the velocity. Therefore, a new hyperbolic trajectory occurs which is governed by the new velocity, the new charge, and the new mass of the final ion.

The increase of velocity was calculated from the Q value deduced from the energy distribution. When distinct peaks appeared, each of them was treated separately with its particular Q value. For continuous energy distributions an average Q was chosen.

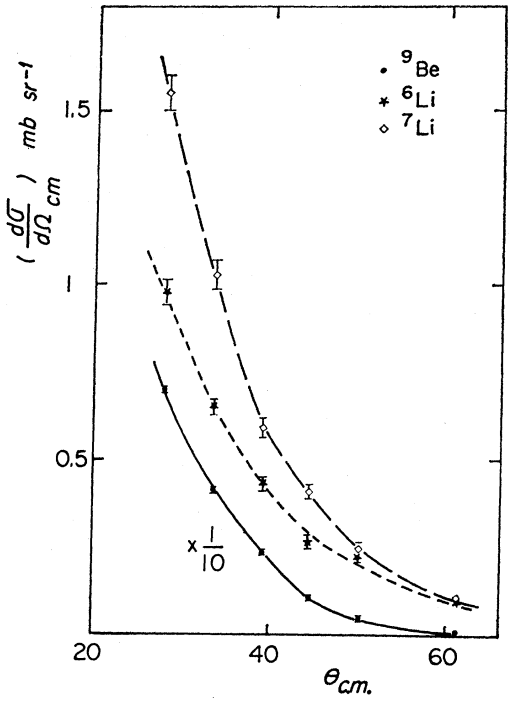

FIG. 9. Angular distributions for Li and Be ions.

For each case, we started with a large set of impact parameters p_i, varying between 0 and 20 F, every 0.1 F. Each impact parameter p_i gave a particular $R_{\min}$ and a well-defined scattering angle $\bar{\theta}$ after the transfer reaction. For this $\bar{\theta}$ value, we took the experimental cross section $d\sigma/d\Omega$ and $(d\sigma/dR_{\min})/(d\sigma/d\Omega)$ was calculated as a function of the impact parameter

$$\frac{d\sigma/dR_{\min}}{d\sigma/d\Omega} = \frac{8\pi}{p_i}\sin^2\tfrac{1}{2}\bar{\theta}\cos\tfrac{1}{2}\bar{\theta},$$

and the probability that the transfer occurs at a distance R follows the relationship

$$d\sigma/Rdr = (8\pi/p_i^2)(1-\sin\tfrac{1}{2}\bar{\theta})\sin^2\tfrac{1}{2}\bar{\theta}.$$

A typical distribution is given in Fig. 11. The maximum value appears at 11.5 F. If one assumes that this

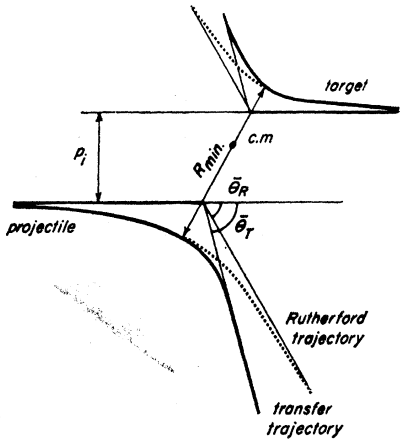

FIG. 10. Treatment of the Coulomb scattering in the center-of-mass system. $\bar{\theta}_T$ is the experimental scattering angle. $\bar{\theta}_R$ is the scattering angle for a pure Rutherford trajectory.

distance corresponds to grazing trajectories when the two nuclei centers are at R_1+R_2, a value of 1.6 F is deduced for r_0.

Table I gives the average values of $R_{\min}$, $\langle R_{\min}\rangle$, at which the cross section is the largest. They are all included between 9 and 12 F. In single-transfer reactions, a value around 11.5 was found for excited levels as well as for ground states, although there is a slight tendency to observe larger values (12 F) for excited levels in ^{13}N and ^{11}B. Low values were found for the lightest products, i.e., Be and Li. It might be concluded that the transfer reaction for a large number of nucleons occurs at closer distances of approach than single-nucleon transfers. On the other hand, we have

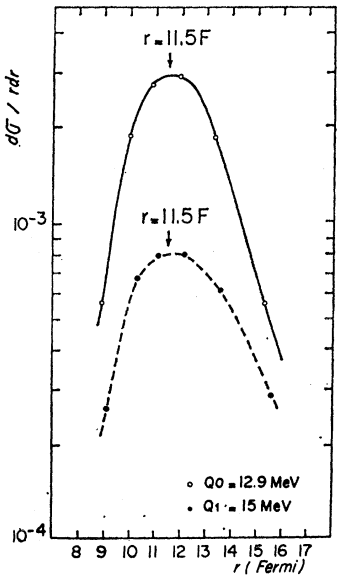

FIG. 11. Angular distributions plotted as $d\sigma/RdR_{\min}$ versus $R_{\min}$ for ^{11}C. Ground state at $Q_0=12.9$ MeV and excited state at $Q=15$ MeV.

TABLE I. Mean value of the distance of closest approach where the yield of transfer process is the largest. $\langle R_{min}\rangle$ values are given for excited states when they are different from the ground-state values (^{13}N*, ^{14}C*, and ^{11}B*).

Nucl after transfer	^{13}N	^{13}N*	^{14}C	^{13}C	^{11}C	^{11}B	^{11}B*	^{10}B	^{9}Be	^{7}Li
$\langle R_{min}\rangle$ F	11.5	12	11	11	11.5	11	11.5	9.5	9	9
r_0 if $\langle R_{min}\rangle = r_0(A_1^{1/3}+A_2^{1/3})$	1.6	1.7	1.55	1.55	1.6	1.55	1.6	1.35	1.3	1.3

not included in the table $\langle R_{min}\rangle$ for ^{15}N, ^{14}N, and ^{14}O*. The treatment described above would lead to values around 13 F, i.e., r_0 of the order of 1.9. These results are contradictory with the data obtained for ^{10}B and for light products, and it is not possible to admit that a large number of nucleons (2 or 3) are transferred at such a large distance of the boundaries of the nuclei. It seems to us that the approximation of a simple perturbation of the Coulomb scattering trajectory is not applicable in these cases. Also, for ^{12}B, $\langle R_{min}\rangle$ is equal to 13 F. Here again the charge exchange (^{12}C–^{12}B) is probably due to a very peculiar mechanism.

We have not been able, during these experiments, to explore small angles. However, since this first set of data, we have carried on some new work with 115-MeV ^{14}N ions. It has been observed that the cross section increased very much at angles below 15°, both for *single-* and *multi-transfer* reactions. A first preliminary angular distribution is shown in Fig. 12 for ^{15}N. Large R_{min} would correspond to very small angles. Therefore, the appearance of large partial cross sections shows that the treatment in R_{min} terms fails at small angles. Rutherford trajectories are not followed all the way and the transfer reaction cannot be considered as a small perturbation. During the process, there should be a large change in the direction of the ion which decreases the scattering angle. A possible mechanism would consist of a temporary fusion of the two nuclei, followed by a fission after a rotation of the compound state.

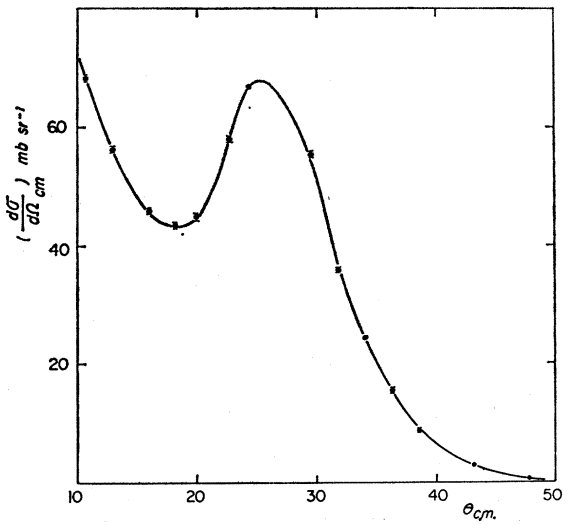

FIG. 12. Angular distribution for the neutron-transfer reaction Ag(^{14}N, ^{15}N).

Coming back to the maxima observed in most of the angular distributions, we have compared our results with theoretical calculations made by da Silveira[12] on the following bases: Scattering waves were treated in

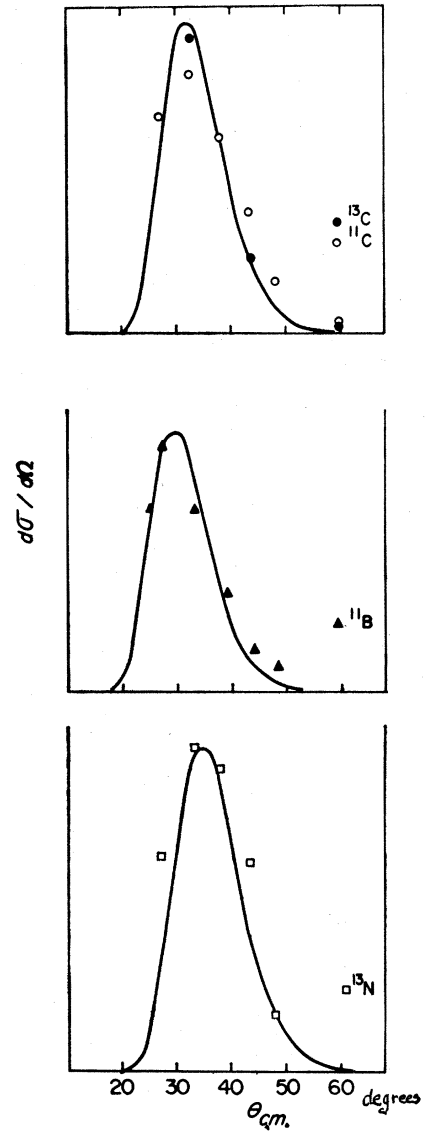

FIG. 13. Comparison between the calculated angular distribution for one-nucleon transfer (curves by da Silveira) and the experimental distributions measured for several single-nucleon transfers. ^{13}C, ^{11}C, ^{11}B, ^{13}N. (The magnitude of calculated cross sections is arbitrary.)

[12] R. da Silvera (personal communication).

TABLE II. Cross sections in mb for various transfer reactions.

Z	Li		Be			B			C			N		
M	6	7	7	9	10	10	11	12	11	13	14	13	14	15
σ	1.0	1.4	0.2	5.0	2.5	3.5	27	0.25	2.6	23.0	1.5	0.45	0.3	0.2
Number of transferred nucleons			$-\alpha$ $-n$	$-2p$ $-n$	$-2p$	$-p$ $-n$	$-1p$	$-p$ $+n$	$-n$	$+n$	$+2n$	$+p$	$+p$ $+n$	$+p$ $+2n$

TABLE III. Cross sections in mb for particular states. Q_0 corresponds to the ground state.

Q values (MeV)	^{11}B		^{11}C		^{13}C		^{14}C				^{13}N		
	$Q_0=8$	Others	$Q_0=13$	$Q=15$	$Q_0=5.0$	$Q=9.0$	$Q_0=4.8$	$Q=7.6$	$Q=11.6$	$Q=14.8$	$Q_0=5.6$	$Q=7.9$	$Q=9.9$
σ	0.7	27	1.4	0.4	5.8	12	0.15	0.1	0.7	0.4	0.07	0.25	0.05

the Glauber[13] approximation, provided that $Q \ll \epsilon$. The perturbation by the target nucleus is done by a potential $V(r)$ made of a Coulomb part $Z_1Z_2e^2/r$ and of the imaginary part of a nuclear potential, $-iw_0 \exp(-\alpha r^2)$, where α and r have the usual values of a Gaussian-type potential. The absorption is described by this term. Figure 13 shows a comparison between the experimental points and the calculated angular distribution after normalization. The agreement is very good for ^{13}C, still satisfactory for ^{11}C, ^{13}N, and ^{11}B.

5. TOTAL CROSS SECTIONS FOR TRANSFER REACTIONS

Although measurements have been made only down to 25°, it seems interesting to integrate $d\sigma/d\Omega$, in order to obtain a lower limit of the total cross section. Even with a large error, the contribution of $d\sigma/d\Omega \sin\theta$ is small at θ lower than 20° and the total error in the cross section might not be very large. Tables II and III give the cross sections. The largest were obtained for ^{11}B $(-1p)$ and ^{13}C $(+1n)$.

The comparison of the cross sections for ^{11}B and ^{13}N shows a ratio $\sigma(-1p)/\sigma(+1p)$ of the order of 60. Since Q_0 value is favorable for ^{13}N (around 4 MeV) as compared with ^{11}B (around 7.5 MeV), it is clear that the Coulomb effect is of great importance. Although our results are in qualitative agreement with the conclusion of Diamond *et al.*,[5] a comparison with Fig. 2 of this paper shows some quantitative discrepancy. It might be due to the fact that the number of available states in the product is important.

At the inverse $\sigma(-1n)/\sigma(+1n)=0.1$. Here the Q_0 value favors ^{13}C (4.5 MeV) as compared with ^{11}C (11.5 MeV), and the absence of Coulomb effect leads to a larger yield for ^{13}C.

The comparison of $\sigma(-pn)$ and $\sigma(+pn)$ made on ^{10}B and ^{14}N leads to the same conclusion of the large part taken by the Coulomb effect since $\sigma(-pn)/\sigma(+pn)=14$, although Q values would favor ^{14}N.

For large multitransfer reactions, the highest yield was observed on ^{9}Be, but we must remember that the transfer of an α particle would lead to unstable ^{8}Be. On the other side, we have been able to estimate that the upper limit for the cross section of ^{16}O is of the order of 1 μb.

As a conclusion we should like to emphasize several points which have been confirmed by our experiments.

First, it has been clearly shown that proton transfers are less probable than neutron transfer when the target is a medium or heavy nucleus. Furthermore, the probability of transferring a proton from the target to the projectile or on the contrary from the projectile to the target, is very much affected by the Q value and the Coulomb energy balance, as was suggested by Diamond *et al.*

Angular distributions of single-transfer reactions present a maximum at a preferential angle which might be explained with the assumption of a scattering process during which the nucleon or cluster transfer occurs without affecting the trajectories very much. Calculations made on models like those of Kalinkin,[14] Frahn and Venter,[15] and Dar[16] may well describe the phenomenon, provided use is made of an adequate "transfer parameter." The data may also be compared with a more elaborate scattering wave theory where the potential is a Coulomb term plus the imaginary part of a Gaussian nuclear potential.

However, both for multinucleon and single-nucleon transfers, a forward peaked contribution has been discovered without any doubt, which must be explained by an additional mechanism.

[13] R. J. Glauber, in *Lectures in Theoretical Physics*, edited by W. E. Brittin and L. G. Dunham (Wiley-Interscience, Inc., New York, 1959), Vol. 1.

[14] B. N. Kalinkin and J. Grabowski, Acta Phys. Polon. **24**, 435 (1963).

[15] W. E. Frahn and R. H. Venter, Nucl. Phys. **59**, 651 (1964).

[16] A. Dar, Phys. Rev. **139**, B1193 (1965).